Protamines: Structural Complexity, Evolution and Chromatin Patterning

Harold E. Kasinsky[1], José María Eirín-López[2] and Juan Ausió[3,*]

[1]*Department of Zoology, University of British Columbia, Vancouver, British Columbia, Canada V6T 1Z4;* [2]*XENOMAR-CHROMEVOL Group, Departamento de Biología Celular y Molecular, Universidade da Coruña, E15071 A Coruña, Spain;* [3]*Department of Biochemistry and Microbiology, University of Victoria, Victoria, British Columbia, Canada V8W 3P6*

Abstract: Despite their relatively arginine-rich composition, protamines exhibit a high degree of structural variation. Indeed, the primary structure of these histone H1-related sperm nuclear basic proteins (SNBPs) is not random and is the depository of important phylogenetic information. This appears to be the result of their fast rate of evolution driven by positive selection. The way by which the protein variability participates in the transitions that lead to the final highly condensed chromatin organization of spermatozoa at the end of spermiogenesis is not clearly understood. In this paper we focus on the transient chromatin/nucleoplasm patterning that occurs in either a lamellar step or an inversion step during early and mid-spermiogenesis. This takes place in a small subset of protamines in internally fertilizing species of vertebrates, invertebrates and plants. It involves "complex" protamines that are processed, replaced, or undergo side chain modification (such as phosphorylation or disulfide bond formation) during the histone-to-protamine transition. Characteristic features of such patterning, as observed in TEM photomicrographs, include: constancy of the dominant pattern repeat distance λ_m despite dynamic changes in developmental morphology, bicontinuity of chromatin and nucleoplasm, and chromatin orientation either perpendicular or parallel to the nuclear envelope. This supports the hypothesis that liquid - liquid phase separation by the mechanism of spinodal decomposition may be occurring during spermiogenesis in these species. Spinodal decomposition involves long wave fluctuations of the local concentration with a low energy barrier and thus differs from the mechanism of nucleation and growth that is known to occur during spermiogenesis in internally fertilizing mammals.

Keywords: Protamines, structure, evolution, chromatin/nucleoplasm patterning, lamellae, spermiogenesis

PROTAMINES: THE POWER OF R

Protamines [1] represent one of the three major groups of sperm nuclear basic proteins (SNBPs) [2]. They can be defined as relatively small proteins of up to 100 amino acids with a highly basic amino acid composition consisting predominantly of arginine ($\geq$ 30% mol arginine/mol protein) [2, 3] (Fig. (**1A**)). Although these proteins are found evenly distributed throughout the protostome and deuterostome branches of bilaterian animals [4], they are often present in organisms at the tips of the phylogenetic tree [5, 6].

During spermiogenesis in the organisms consisting of the protamine SNBP type, histones are gradually replaced by protamines (Fig. (**1B**)). During the process, chromatin undergoes one of its most dramatic structural transitions, from a highly dynamic histone-mediated nucleosome organization to a highly stable and compact nucleoprotamine organization in the mature sperm. In the nucleosome arrangement, about 200 bp of genomic DNA are coiled around a histone core but only about 10% of the positive charge contributed by the histones forms electrostatic interaction with the DNA phosphates [7, 8]. Linker histones (H1 family) bind to the linker DNA connecting adjacent nucleosomes, providing additional charge neutralization of these regions and assisting with the compaction of the chromatin fiber [9]. By contrast, protamines in the mature sperm interact with DNA in a linear fashion with all their arginines interacting with the phosphate side chains [3, 10].

The detailed mechanisms involved in the nucleohistone to nucleoprotamine chromatin transition during spermiogenesis are still poorly understood, but they are assisted by chromatin remodeling complexes [11], highly germ line specific histone variants [12-15] and post-translational modifications (PTMs) of the chromosomal proteins involved. Histones become highly acetylated (especially histone H4) in both vertebrate [16] and invertebrate organisms [17], and in vertebrates they are also ubiquitinated previously to protamine displacement [18]. Protamines are phosphorylated at the onset of the histone displacement. Histone acetylation enhances the dynamics and lowers the stability with which histones interact with DNA, facilitating the displacement by protamines [16], and histone ubiquitination has been recently shown to regulate nucleosome removal [19]. Protamine phosphorylation plays a critical role in their proper deposition onto the DNA template [4], is likely to be involved in chromatin patterning [20] and possibly participates in their removal during early fertilization.

The high abundance of arginine in protamines when compared to histones or to other SNBPs and the gradual replacement of lysine by arginine observed in the protamines of the organisms in the most evolutionarily advanced groups

*Address correspondence to this author at the University of Victoria Department of Biochemistry, Petch Bldg., Room 258, Victoria, BC, V8W 3P6, Canada; Tel: 1-250-721-8863; Fax: 1-250-721-8855;
E-mail: jausio@uvic.ca

0929-8665/11 $58.00+.00

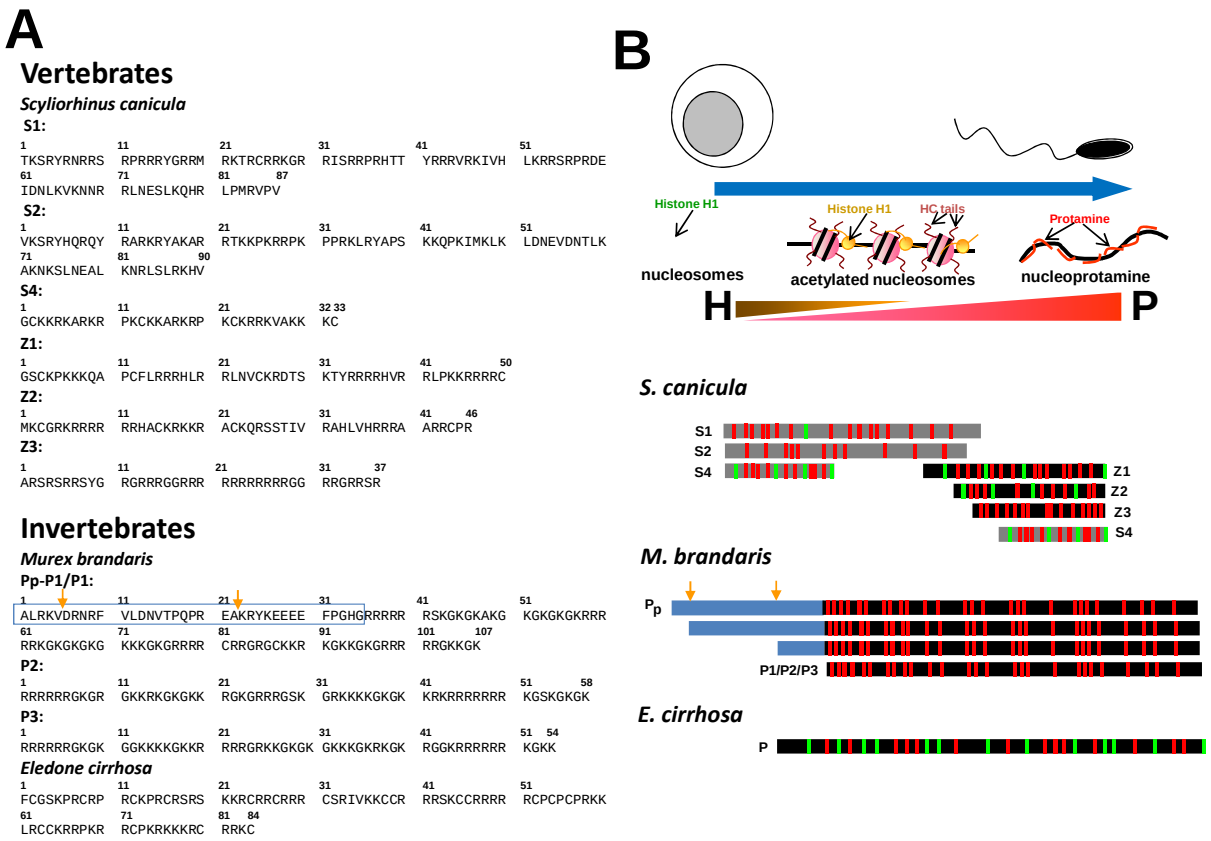

Figure 1. *Vertebrate and invertebrate protamine diversity and complexity.* **A)** Amino acid sequences of a few examples of vertebrate and invertebrate protamines. Vertebrates: chondrychthyan fish, *Scyliorhynus canicula* (dogfish) intermediate proteins S1 (P13275) and S2 (P11020), protamine Z3 (P30258) and keratinous protamines Z1 (P08433), Z2 (P06841) and S4 (P30259) [88, 90]. Invertebrates: cenogastropod, *Murex brandaris* (murex snail) molecular precursor Pp-P1 (P83211) of protamine P1 [76, 77]. The box highlights the leading sequence and the orange arrows indicate the sites of post-translational cleavage (processing) leading to the mature protamines P1, P2 (P83212), and P3 (P83213) found in mature sperm; cephalopod, *Eledone cirrhosa* (horned octopus) keratinous protamine (P83183) [36]. The name keratinous refers to the presence of cysteine [144]. **B)** The upper part shows a schematic illustration of the chromosomal protein and chromatin transitions that take place during spermiogenesis in those organisms that contain protamines in their spermatozoa. H: histones; P: protamines. The lower section provides a schematic representation of the structural complexity of the protamines chosen as an example. The red bars indicate positively charged amino acids (lysine or arginine) and the green bars indicate cysteine. The blue region in *M. brandaris* Pp corresponds to the protamine leading sequence that is post-translationally cleaved (orange arrows) during maturation.

of organisms [3], especially in those with internal fertilization [21, 22], is not surprising. Whereas in the somatic cells chromatin must adopt a highly dynamic organization suitable to the nuclear metabolic processes such as DNA replication, recombination, repair and transcription, in the spermatozoa chromatin adopts a tightly packed static conformation designed to compact chromatin as much as possible within the nucleus. This assists the highly specialized sperm cell in acquiring a streamlined hydrodynamic shape [21], while protecting the genome from exogenous damaging agents [23]. In this regard, the higher hydrogen bonding potential of arginine [24, 25] over lysine appears to have been selected by protamines in order to preferentially increase their affinity for DNA [26].

The highly stable structural constraints imposed by protamines on the genomic DNA as histones are being displaced during spermiogenesis led initially to the belief that transcription ceased during this process [27]. However, there is now increasing evidence for post-meiotic expression of specific genes in both invertebrate and vertebrate organisms [28-31]. To account for this, it has been proposed that the histone-to-protamine chromatin transition may take place in a very orderly fashion [32]. Indeed, there is some initial experimental evidence supporting this notion. Any DNA metabolic activity on a highly electrostatically neutral nucleoprotein substrate, such as that resulting from the association of DNA with such very arginine-rich proteins as protamines would otherwise be very difficult to explain.

STRUCTURAL COMPLEXITY OF PROTAMINES

Despite their relatively simple amino acid composition (Fig. (**1A**)), protamines exhibit a high extent of diversity at the primary structure level. In addition, their high basic amino acid contents does not prevent them from adopting under certain conditions, such as in the presence of helicogenic solvents [33] or upon interaction with DNA, a considerable extent of secondary structure organization; hence they fall within the category of intrinsically disordered proteins [34, 35].

The additional presence of cysteine, an amino acid which is otherwise absent in other SNBPs, in certain protamines adds structural complexity to this group of chromosomal proteins. In fact, it is interesting to note that in the protamines of the most evolved groups of protostomes and deuterostomes such as the cephalopods [36] (Fig. (**1**)), the dipteran insects (*Drosophila*) [37] and eutherian mammals [38], an increase in the cysteine composition is observed. Cysteine has also shown to be present in the sperm proteins of chondrychthyans, a rather primitive group of cartilaginous fish [39] (see (Fig. (**1**)). The presence of cysteine, in addition to a high basic amino acid content, may assist in the formation of a tighter sperm chromatin condensation following oxidation of the thiols to produce disulfide bridges between neighbouring protamines [36, 40] and/or intra-protamine bridges [41]. A recent report in humans indicates that there is at least one zinc molecule for every protamine [42], providing additional evidence for zinc also forming bridges with individual protamine thiol groups in these organisms [43, 44].

Another level of structural complexity arises from the differences in size of the protamines within and across different species and from the presence of intra-specific microheterogeneity [15, 23] (see Fig. (**1B**), *M. brandaris* P1-P3). As well, in many instances within representatives of the two bilaterian branches, protamines undergo a complex pattern of processing that involves multiple post-translational cleavage (see Fig. (**1B**)), *M. brandaris* Pp-P1) [4]. This process plays an important role in the protamine deposition [45] process and patterning [20] during spermiogenesis.

The role of the high structural inter- and intra-species variability of protamines is reflected in the high evolutionary rate exhibited by these proteins [4, 46-48] (see the following two sections of this paper). This is in high agreement with the fast rates of evolution observed in other reproductive proteins [49], including other chromosomal proteins such as some of the highly specialized histone variants (*i.e.* histone H2A.Bbd) associated with the spermiogenesis process in mammals [14]. This high protein diversity contrasts with the highly conserved nature of the mechanisms and genes [50] involved in other fundamental aspects of the spermatogenic process. For instance, proteins such as the bromodomain testis-specific (BRDT) or the ubiquitin ligase, ring finger 8 (RNF8) exhibit a considerable extent of conservation. These proteins participate in histone ubiqutination [19] and acetylation [51] processes which are essential for the histone to protamine transition. Similarly, members of the deleted-in-azoospermia (DAZ) gene family of RNA binding proteins are equally [52] conserved. All of this raises the intriguing question as to what is the reason for such structural diversity and variability. Protamines have been shown to provide a fertility [53] and competitive intra- and inter-specific edge to certain organisms [38]. However, transgenic mice having cysteine containing protamines and expressing a chicken protamine (which lacks any cysteine) were found to be fertile [54]. Thus the precise molecular implications arising from the extensive protamine structural diversity still remain largely unknown.

An equally intriguing question is that of the different types of chromatin organization [globular [55], lamellar (this paper), toroidal [56]] that precede the formation of the highly compact chromatin organization in the mature sperm during the late stages of spermiogenesis. Here again, the mechanisms leading to these different organizations are not well understood. In many instances these diverse transitional chromatin conformations are observed in organisms with seemingly closely related protamine sequences and vice versa. The last section of this paper describes the fundamental mechanics involved in lamellar patterning. This represents a chromatin re-organization that leads to a highly compacted sperm nucleus that is widespread in many organisms and, as depicted in (Fig. (**1**)), can arise from protamines exhibiting a seemingly structural disparity.

HISTONE H1 AND THE EVOLUTION OF SNBPS

Although the evolution of the histone multigene families has been classically described as a concerted evolution process based on the extensive homogenization of sequences through a rapid process of interlocus recombination and gene conversion [57], such an hypothesis has been discarded given the increasing diversity of histone variants identified during the last decade [58]. Instead, evolutionary studies taking advantage of the great flow of molecular data coming from genome projects have revealed that, far from a notion of homogeneity, the long-term evolution of histones is based on the generation of genetic diversity through a mechanism of birth-and-death evolution based on recurrent gene duplications subject to purifying selection at the protein level [59, 60]. Such a mechanism has been responsible for the structural diversification and functional differentiation leading to the broad histone diversity involved in the progressive increase in the complexity of the chromatin structure and metabolism during evolution [61].

The evolutionary mechanism of birth-and-death is especially well illustrated by the histone H1 family, which displays the highest level of diversification amongst histones. The H1 family promotes the differentiation of variants specific to somatic and germinal cell lineages encompassing specific functions both in chromatin packaging and dynamics [62], as well as in reproduction-associated traits, including sperm shape and motility, fertilization and reconstitution of somatic chromatin in the zygote after fertilization [2, 63]. (Fig. (**2A**)) displays the evolutionary process leading to the differentiation of the lineages encompassing histone H1 and SNBPs in different metazoan groups, sharing a common evolutionary origin from an ancestral replication-independent (RI) histone H1 very early in metazoan evolution [5]. The differentiation between somatic and germinal cell lineages later on resulted in a functional specialization, thereby leading to a segregation between replication-independent (RI) and replication-dependent (RD) somatic H1 histones, as

well as to the transition towards highly specialized arginine-rich protamines (P) through a protamine-like (PL) intermediate during the evolution of SNBPs in the germ lineage [5, 64]. Indeed, the evolutionary ancestry shared by RI H1s and SNBPs of the P-type is reinforced by their common structural and functional features, which contrast with those of RD H1 proteins, and include the following: encoding by low copy number genes located at solitary genomic positions, transcription through polyadenylated mRNAs and involvement in heterochromatinization of terminally differentiated proteins [3, 5].

In the case of the somatic H1 lineage, recurrent gene duplications of an ancestral RI histone H1 eventually led to the differentiation of a new group of RD H1 genes. However, while the RD group acquired a role encoding canonical histones needed in large amounts during the S-phase of the cell cycle, the RI group held onto a basal role encoding specialized H1 variants expressed constantly but at low levels during the cell cycle [59, 62, 65]. Such differentiation between both somatic lineages occurred early in metazoan evolution, before the split between protostomes and deuterostomes. It encompasses a genetic diversification process without drastic changes in their overall protein structure, through a birth-and-death process under strong purifying selection acting at the protein level [62]. Furthermore, the subsequent functional differentiation between RD and RI H1 lineages ran in parallel across both groups of metazoans, as assessed by the presence of RI and RD representatives in both groups of organisms (Fig. (**2A**)).

On the other hand, the differentiation of a germinal cell lineage encompassing the ancestral RI histone H1 lineage allowed for the origin and differentiation of SNBPs later on during evolution, based on a mechanism of gene duplication and selection as well [2, 3, 63]. However, and quite to the contrary, in the case of somatic H1s, the evolution of SNBPs involved a progressive reduction in structural protein complexity. Accordingly, the ancestral SNBPs belonging to the lysine-rich histone type (H-type) were responsible for the differentiation of the highly specialized arginine-rich protamines (P-type) through a lysine/arginine-rich protamine-like (PL-type) intermediate. However, this process first involved the functional segregation of the different domains (N-terminal, globular and C-terminal) in the ancestral H1 proteins, and the appearance of the first PLs, such as PL-I [2, 63], whose physical segregation later on led to the differentiation of the more specialized SNBP components (PL-II, PL-III, Pl-IV) [5]. In this scenario, it has been proposed that the origin of arginine-rich protamines would have resulted from a process involving a frameshift mutation in the lysine codons of SNBPs of the PL type corresponding to the C-terminal region of H1, leading to the transformation of lysine residues to arginine residues [66, 67]. The differentiation among the three SNBP lineages must have also occurred early in metazoan evolution before the split between protostomes and deuterostomes, allowing for the parallel differentiation of H, PL and P-types across both metazoan lineages [5, 66, 67].

Overall, both histone H1 and SNBPs follow a common evolutionary trend which is characterized by their diversification early in metazoans and their parallel differentiation across protostomes and deuterostomes. Furthermore, such a process is translated into a higher level due to the presence of parallel evolution between the somatic and the germinal cell lineages. This process constitutes what has been coined the "histone hypothesis for the vertical parallel evolution of SNBPs" [2, 3, 5, 63, 66].

TRACING THE FOOTSTEPS OF RAPIDLY EVOLVING ARGININE-RICH PROTAMINES

Protamines, which represent the highest level of specialization among SNBPs, are present in the sperm of both protostomes (such as molluscs) and deuterostomes (including tunicates and chordates). In these organisms the histones from the progenitor germ cells at the onset of spermatogenesis are replaced by protamine in the late stages of spermiogenesis [16]. Protamines are small and highly variable proteins, encompassing high contents of arginine (more than 30%). Thus, their high charge density allows them to bind DNA with high affinity and to more efficiently shield the charges on the DNA phosphate backbone. Compared to somatic histones, this results in maximal compaction of the genome [15].

Despite their high level of structural heterogeneity, the amino acid distribution in the primary structure of protamines does not seem to be random. Indeed, their amino acid sequence still stores very valuable phylogenetic information, due to the fact that they are subject to positive (adaptive) selection [15, 16] that is responsible for their rapid evolution. This is similar to other reproductive proteins [49]. The arginine-rich P-type has probably been selected in the course of evolution of the vertebrates due to constraints imposed by internal fertilization [68]. However, the selective process has been focused on maintaining high arginine levels, regardless of the actual positions occupied by these residues in the molecule [69]. We have already shown that this information can be successfully used in phylogenetic inference, including the cases of stickleback fish species [46], teleost fishes [68], birds and reptiles [6, 70] and different groups of mammals [71, 72].

The phylogeny shown in (Fig. (**2B**)) displays the evolutionary relationships estimated by maximum likelihood among protamines from different metazoan lineages, especially for the case of fishes, in which more information is available. Accordingly, the occurrence of protamines is seen in protostomes such as molluscs, as well as in vertebrates as ancient as sharks and other cartilaginous fishes. However, protamines are also present in bony fishes. H-type and PL-type SNBPs are also represented in the sperm of organisms from this group, unlike the case of chondrychthyes in which SNBPs are exclusively of the P-type [73].

While the present phylogeny seems to fit well with the taxonomic relationships among the different lineages analyzed at a local level (within groups), relationships between the more general taxonomic groups indicated on the right margin of the tree (Fig. (**2B**)) seem to be somewhat unresolved by the present topology. This is most likely due to the saturation in the amino acid substitutions, as well as the selection for arginine content, instead of selection for maintaining the positions of arginine residues. However, it is possible to clearly discriminate a monophyletic group encompassing

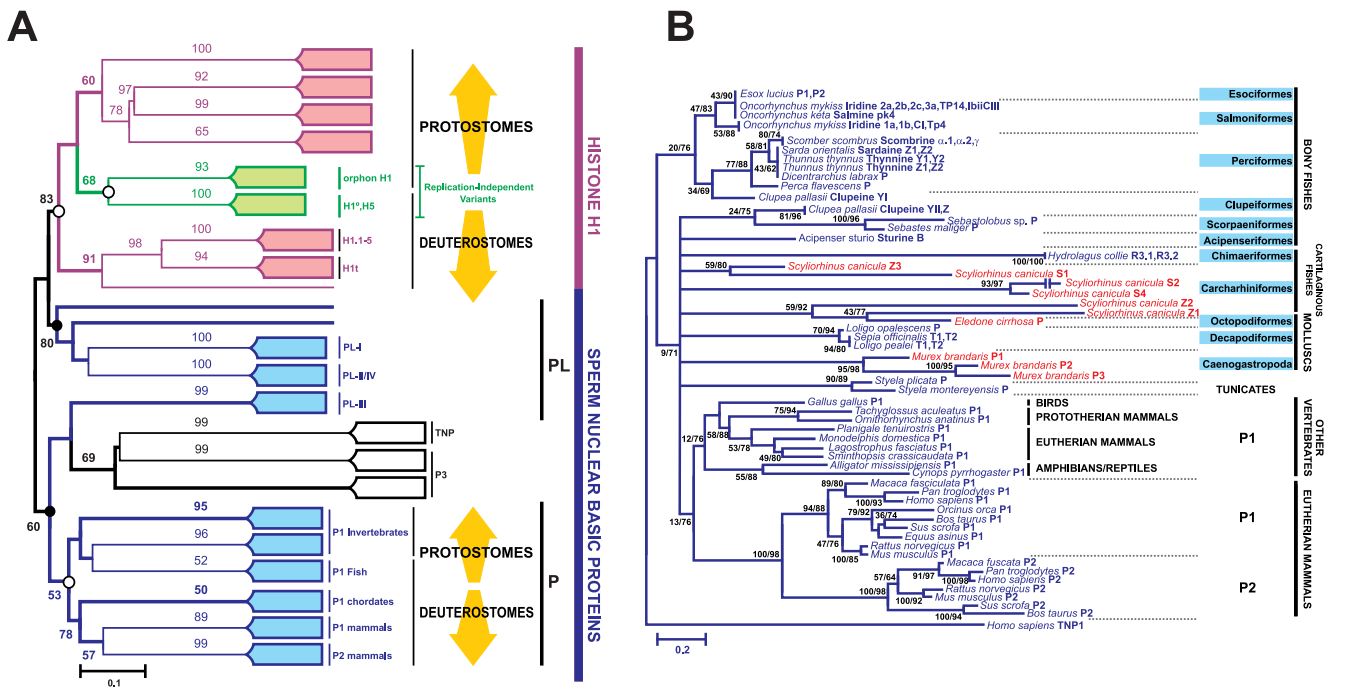

Figure 2. *Evolution of SNBPs and protamines*. **A**) Simplified protein phylogenetic relationships between histone H1 and SNBPs based on uncorrected *p*-distances [adapted from [5]]. The numbers for interior branches in the unrooted topology represent BP values based on 1000 replicates and are only shown when greater than 50%. "BP values" stands for "bootstrap values" in the tree. These values represent a quantitative measure of the reliability of the groups defined by the topology of the tree The monophyletic origin of H1 histones of the RI lineage and that of protamines is indicated by open circles, while the polyphyletic origin of PL proteins is indicated by black circles. Taxonomic groups and different histone and SNBP subtypes are indicated on the right side of the topology. **B**) Maximum likelihood phylogeny reconstructed from protamine amino acid sequences belonging to different metazoans using the JTT model of protein evolution. "JTT" stands for the name of the authors in reference [144]. The numbers for interior branches represent non-parametric bootstrap (npBS) probabilities based on 100 replications followed by approximate likelihood ratio test (aLRT) values. These are only shown when at least one of the values is 50%; otherwise branches were collapsed. Numbers near species indicate the type of protamine. Taxonomic groups are indicated in the right margin of the tree. The transition protein 1 from humans (TNP-1) has been used to root the tree.

fishes, amphibians and non-eutherian mammals. It has been suggested that the driving force behind this evolution in fish and amphibians may be differing constraints placed on the sperm by internal versus external fertilization [21, 22]. Following the appearance of amniotes, all organisms contain protamines in their sperm, which may suggest an evolutionary trend towards the use of protamines to package sperm DNA in taxa located at the uppermost tips of evolutionary branches [2, 3, 63].

The topology displayed in (Fig. (**2B**)) suggests that the present analysis is valid in providing a deeper insight into the evolution of mammalian protamines, which represent a highly supported monophyletic group. In particular, protamines from eutherians are clearly differentiated from those of metatherians and prototerians, as well as from protamines from reptiles and birds. Two types of protamines are found in mammals (P1 and P2). However, while P1 has been found in all mammals, P2 is exclusively expressed only in a few eutherians, including human and mouse [53]. Indeed, the phylogeny from (Fig. (**2B**)) also supports a common origin for eutherian P1 and P2 protamines, with the slightly more recent appearance of the P2 type likely arising by gene duplication of a P1 precursor [74]. In mammals cysteine is present in both P1 and P2 eutherian lineages, and is also present in some marsupial P1 protamines, where this residue was incorporated by a process of convergent evolution [75].

PROTAMINES AND SPERMIOGENIC CHROMATIN PATTERNING

In (Fig. (**1**)) and (Fig. (**2B**)), we have highlighted a small subset of invertebrate protamines from two species of internally fertilizing molluscs that are associated with the histone-to-protamine transition during chromatin/nucleoplasm patterning in the early and middle steps of spermiogenesis. This includes the arginine-rich pro-protamine Pr-P1 of the muricid neogastropod *Murex brandaris* that is processed by serial proteolysis in the spermatid nucleus, to protamines P1, P2 and P3 in the nucleus of the mature sperm [76-78]. In addition the cysteine-rich keratinous protamine of the octopus *Eledone cirrhosa* is also highlighted [36].

How might the processing and side chain modification of such protamines be related to the dynamic chromatin changes that characterize spermatid nuclear patterning and subsequent condensation in these invertebrates, as well as in an internally fertilizing vertebrate, the cartilaginous fish *Scyliorhinus canicula* (Fig. (**1**))?

In 2005, Harrison *et al*. [79] presented the hypothesis that the dynamic mechanism of liquid-liquid unmixing involving phase separation by spinodal decomposition might explain the development of dramatic patterns of chromatin/ nucleoplasm during spermiogenesis in the snail *M. brandaris*. In this species, patterning is from granules to fibrils to lamellae in early and middle spermatids. However, in the octopus *E. cirrhosa*, post-lamellar patterning is seen as an inversion from chromatin as a dispersed phase to nucleoplasm as a dispersed phase [36, 79]. These patterns can be observed by transmission electron microscopy (TEM) of testis fixed in glutaraldehyde (GLUT-fixed) and stained with metals.

In 2009, Martens *et al*. [20] confirmed the observation of chromatin/nucleoplasm patterning during early spermiogenesis in another internally fertilizing muricid marine snail, *Nucella lamellosa*, using high pressure freezing (HPF) of testis to avoid possible artifacts of the method of fixation. Extending the suggestion of Harrison *et al*. [79], these authors proposed a possible temporal correlation between pattern formation due to spinodal decomposition and the processing of pro-protamine (Fig. (**1**)), including modification by phosphorylation of serine and threonine residues and subsequent dephosphorylation, as also occurs in the muricid snail *M. brandaris* during the coalescence of lamellae [2].

Spinodal decomposition is a physicochemical model involving kinetic, equilibrium and structural aspects of a system en route to equilibrium [79], not out of equilibrium as in Turing's [80] reaction-diffusion mechanisms, which form patterns in milliseconds rather than days, as in spermiogenesis. The classical theory for spinodal decomposition was formulated by Cahn [81] in 1965 in order to explain transient patterning observed in glass during a cold quench from high temperature. It is a mechanism for the separation of two liquid phases with transient pattern being produced in the unstable state by gradually growing concentration inhomogeneity involving "small long-wave fluctuations of the local order parameter such as the local concentration" [[82], p.5]. According to the late Dr. L.G. Harrison (personal communication), spinodal decomposition occurs "on a supramolecular scale of distances in a solution and dealing with concentrations rather than single molecules. But it leads to the idea that molecular changes must be happening where one sees changes in patterning happening".

In the case of spermiogenic chromatin/nucleoplasm patterning, a change from a single phase to two phases can be brought about by the isothermal [83, 84] replacement of histones by protamine through processing of pro-protamines (Fig. (**1**)), and modifications of protamines such as phosphorylation for *M. brandaris* or disulfide bond formation for *E. cirrhosa*, rather than by the more classical route of a temperature shift [[82], Fig. **1.1**].

Characteristic features of spinodal decomposition observed [79] in the early and middle patterning steps of spermiogenesis include: constancy of the dominant pattern repeat distance despite dynamic changes in developmental morphology; bicontinuity (interconnectivity [82]; mutual connectivity [83]) of chromatin and nucleoplasm at the lamellar step, where "the electron dense chromatin and the clear nucleoplasm each appears to be continuous, rather than as one continuous phase and one disperse phase" [[20], p.1403]; and orientation of chromatin either parallel with or perpendicular to the nuclear envelope [[79], Fig. **7**].

The patterning stage of spermiogenesis is then followed by a condensation stage, in which there is a shrinkage of the dominant unit of pattern and the formation of very electron dense, homogeneous chromatin. This is also observed in the internally fertilizing homopteran insect *Philaenus spumarius* [79, 85]. This second stage is probably a phase separation by an ionic crystallization [79].

PROTAMINES AND LAMELLAR-MEDIATED CHROMATIN CONDENSATION IN DOGFISH SPERMATIDS

Are protamines also involved in phase separation by spinodal decomposition as a mechanism for spermatid nuclear patterning in vertebrates? We have analyzed spermiogenesis, for the first time, in the internally fertilizing dogfish (or spotted catshark) *Scyliorhinus canicula* [86] (formerly *Scyllliorhinus caniculus* [87]), based on the TEM photomicrographs of Gusse and Chevaillier [86].

In *S. canicula* (Fig. (**3**, left)), dynamic chromatin patterning during spermiogenesis from granules to fibers to lamellae looks remarkably like that in *M. brandaris* [76-79]. In this species of cartilaginous fish histones are replaced by spermatid-specific basic intermediate proteins that, in turn, are replaced by a protamine and three keratinous protamines [88]. Histones are still present in a section of dogfish testis that is enriched in young spermatids [86, 89], but intermediate proteins S1 and S2 also appear [86, 88]. These two intermediate proteins are less basic than protamines (Fig. (**1**)) and have a molecular mass intermediate between histones and protamines.

Intermediate proteins S1 and S2 are in turn replaced by Z3, a typical fish protamine (see [88] and references therein) and three keratinous protamines: Z1, Z2 and S4, without any proteolytic processing of a protamine precursor.

Protamine Z3, as well as keratinous protamines Z1, Z2, S4, first appear in chromatin lamellae [86, 89] during the patterning stage of spermiogenesis (Fig. (**3**)). The first appearance of S1 and S2 occurs just before this, when the nucleus begins to elongate and displays parallel fibrillar patterning. These data suggest that there may be a correlation between the timing of protamine appearance, disulfide bond formation (keratinisation), (Fig. (**3,** left)), and the timing of chromatin patterning during *S. canicula* spermiogenesis.

Intermediate nuclear basic proteins S1 and S2, protamine Z3, and keratinous protamines Z1, Z2, S4 are also provided with serine side chains for phosphorylation and dephosphorylation [88, 90]. S1 and S2 can be mono-phosphorylated and S1 can also be di-phosphorylated during the patterning stage of spermiogenesis (Fig. (**3**)).

Keratinous protamines Z1 and Z2, and protamine Z3, can be mono-, di- and tri-phosphorylated respectively. These phosphorylations also occur during the patterning stage of spermiogenesis. However, from the sections of the testes examined [86, 89], it is difficult to tell precisely when the dephosphorylation occurs. Likely, this is later on, during the

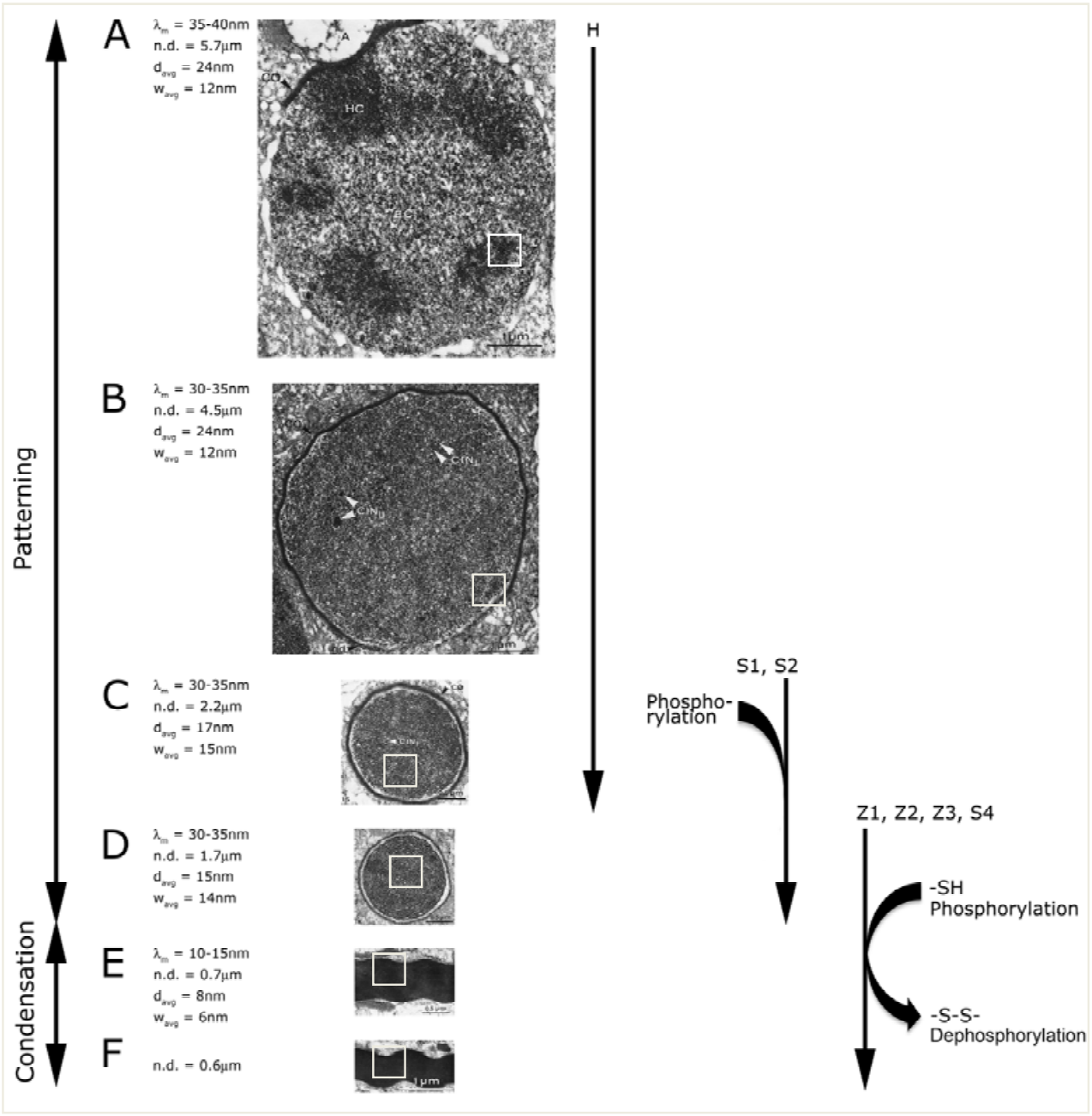

Figure 3. TEM photomicrographs (left), all at the same magnification, of transverse sections showing steps in the patterning and condensation stages within a developing spermatid nucleus of the dogfish *S. canicula*, TEM photomicrographs (at differing magnifications) have been taken from the 1978 paper of Gusse and Chevaillier [86], Fig. **1**, **6**, **15**, **18**, **24**, **25**]. Note the concomitant appearance (right) of histones (H) [13], intermediate proteins (S1, S2) [88, 89] and protamines (Z1, Z2, Z3, S4) [88-90]. Symbols to the left of the TEM photomicrographs are defined in (Fig. (**5,** left). White boxes are shown at higher magnification in Fig. (**4**)). **(**Fig. (**3E, F**)) has been magnified even further in [[86], Fig. **26**].

condensation stage, when disulfide bonds are also formed in the keratinous protamines Z1, Z2 and S4 (Fig. (**3**)).

Is the developmental morphology seen in TEM photomicrographs (Fig. (**3**)), as well as the timing of the histone-to-protamine transition, consistent with the hypothesis of phase separation by spinodal decomposition during spermiogenesis in *S. canicula*?

We look first at the appearance of bicontinuity in TEM photomicrographs of dogfish spermatids (Fig. (**4**, left column)), magnified from (Fig. (**3**)), as well as at the time evolution of a polymer dispersed liquid crystal (PDLC; (Fig. (**4**, center column)).

We start by examining a sketch of 1/interaction parameter χ (chi) – concentration (C), the phase diagram for a sys-

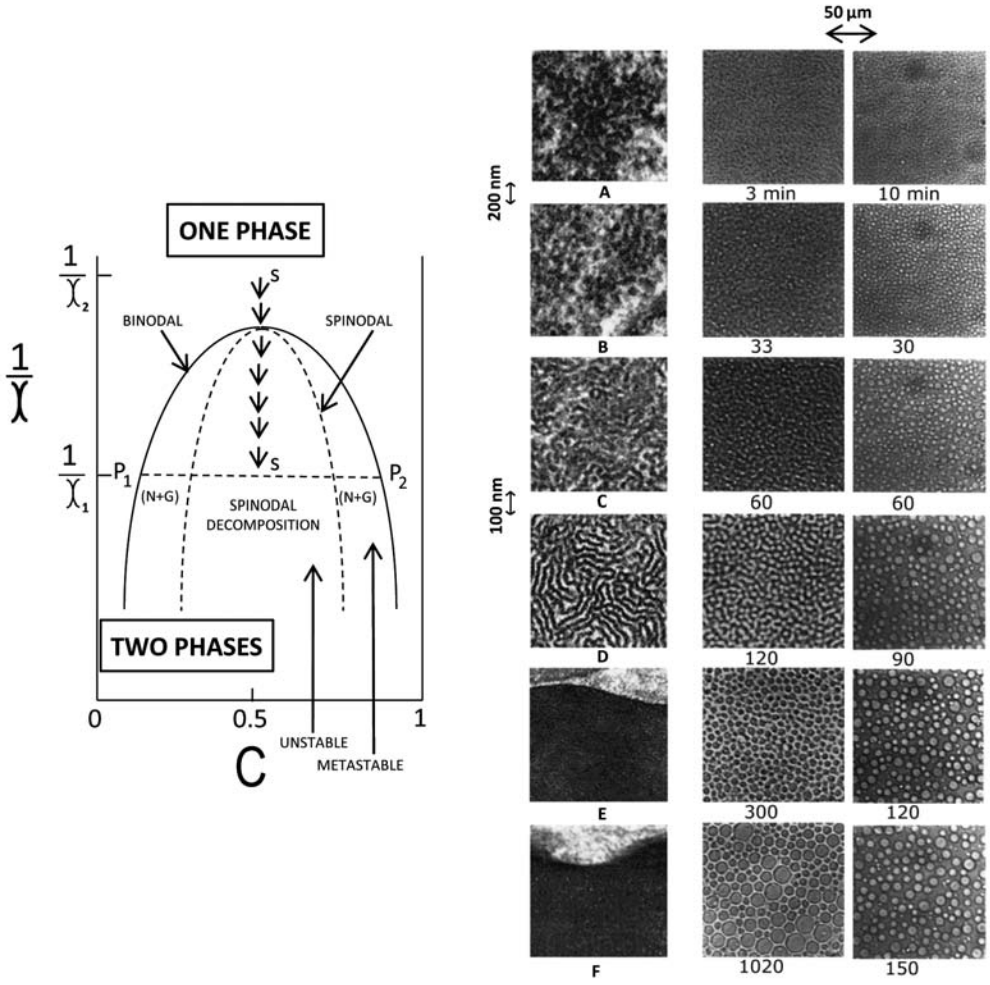

Figure 4. Comparison of spinodal decomposition in TEM photomicrographs of *S. canicula* during spermiogenesis (left column) [86], with polarized optical photomicrographs of the time evolution of a thermally quenched polymer dispersed liquid crystal (PDLC) undergoing either spinodal decomposition (center column: 40/60 wt %) [[91], Fig. **2**] or nucleation and growth (right column: 60/40 wt %) [[91], Fig. **3**]. A sketch of 1/interaction parameter χ (chi) – concentration C, the phase diagram [[93], Fig. **3.5**] for a system of two components (A and B) is shown on the left, where χ is the energy change "when a molecule of A is taken from an environment of pure A and put into an environment of pure B" [[93], p.28], so that χ "expresses the strength of the energetic interaction between the components". C is the concentration, represented as the mole fraction of A running from 0 to 1 ([79], Fig. **10**). In the phase diagram on the left, the composition S changes from a value of $1/\chi$ (sub 2) for a single phase to a value of $1/\chi$ (sub 1) for compositions P1 (B-rich phase) and P2 (A-rich phase) that places the system into the unstable region where it separates into two phases by spinodal decomposition [[79], Fig. **10**]. Such a separation can occur isothermally during spermiogenesis in *S. canicula* (*left* column; TEM photomicrographs here have been magnified from (Fig. (**3**), white boxes), or during the time evolution of a cold quenched 40/60 wt % PDLC (*middle* column) [[91], Fig. **3**]. For the latter $1/\chi$ can be replaced by T (absolute temperature) in the phase diagram on the left. During a cold quench of a 60/40 wt % PDLC into the metastable regions of the phase diagram, nucleation and growth occur (*right* column) [[91], Fig. **2**]. The polarized optical photomicrographs in the *middle* and *right* columns have been taken from the 1996 paper of Kyu *et al.* [91], with the permission of the American Chemical Society.

tem of two components (Fig. (**4**, left)). We plot $1/\chi$ on the vertical axis rather than the more classical temperature because, according to Harrison *et al*. [[79], Fig. **10**]: "Similar behavior can occur in a system of more than two components, and as a result of, e.g., a chemical change in the system rather than change of temperature." Thus, spinodal decomposition can occcur isothermally [83, 84] in the unstable region of the phase diagram (Fig. (**4**, left)), as seen by TEM photomicrographs for spermiogenesis in *S. canicula* in (Fig. (**4**, left column)). It can also be observed in optical light photomicrographs for a 40/60 wt % PDLC after thermal quenching in (Fig. (**4**, center column)). This is a PDLC that consists of 40 wt % polymethyl methacrylate with hydroxyl groups in the liquid form / 60 wt % E7, a mixture of nematic liquid crystals (that includes derivatives of cyanobiphenyl, oxycyanobiphenyl and cyanoterphenyl) with a broad nematic temperature range [[91], p. 204]; [[92], p. 943].

The typical appearance of bicontinuity [83] is readily apparent for both the magnification of step D in the patterning stage of spermiogenesis in *S. canicula* (Fig. (**4**, left column)), as well as at 120 minutes for the 40/60 PDLC (Fig. (**4**, center column)). Such bicontinuity lasts for a few hours in the PDLC [[91], p.208]. How long it lasts in *S. canicula* spermiogenesis is not known.

Such bicontinuity is, however, typical for spinodal decomposition, as compared to nucleation and growth for the 60/40 PDLC after thermal quenching, where droplets are observed in (Fig. (**4**, right column)) due to Ostwald's ripening mechanism [93]. As Kyu *et al*. state, regarding bicontinuity in the 40/60 PDLC [[91], p.206], "This interconnected structure is reminiscent of a spinodal structure. The length scale of this structure increases with elapsed time and eventually the pattern transforms into droplet morphology probably driven by surface tension." We should also point out that, according to the phase diagram of Kyu *et al.* [[91], Fig. **1**], we are comparing only the liquid - liquid phase separation for both *S. canicula* spermiogenesis and for the 40/60 PDLC, not the isotropic liquid - nematic phase separation.

We can see, then, that spinodal decomposition is morphologically similar in appearance whether we are at the nanometer scale of phase separation for chromatin/nucleoplasm during spermiogenesis in *S. canicula* or at the micrometer scale of phase separation in a PDLC.

Second, we can see in a transverse section of step D of *S. canicula* spermiogenesis in both (Fig. (**3**)) and its magnification in (Fig. (**4**)), that all lamellae are oriented to the nuclear envelope in a parallel manner. This is different than in the muricid snail *M. brandaris* [76-78], where all lamellae in a transverse section run perpendicular [79], Fig. **9**] to both the nuclear envelope and the axoneme. This is also the case for another muricid snail, *N. lamellosa* [[20], Fig. **2**]. According to Harrison *et al*. [[94], Fig. **6.1**], this is due to the fact that membranes around these organelles provide a barrier to diffusion since they are located at the boundary of a patterning system. Here the concentration profile is flat [[79], Fig. **7**].

We can speculate that perhaps the parallel orientation in *S. canicula* is the one of lowest energy and that the presence of an additional membrane bound axoneme in the spermatid nucleus of the muricid snails prevents this parallel orientation, thus facilitating a perpendicular orientation. The important point is that the orientation of lamellae in parallel to the nuclear membrane provides evidence for the diffusive instability that is known to be associated with spinodal decomposition [93, 95].

Furthermore, we recognize that the presence of a nuclear matrix in spermatids of *S. canicula* would provide an additional barrier to diffusion. However, if the model for DNA constraint in spermatids of mammals by attachment to the nuclear matrix at many MAR sites [96] also holds for *S. canicula*, then the size of the DNA loops constrained by the matrix, about 50 Kb, may be too large to act as an effective barrier to difffusion.

In order to verify this, it would be necessary to examine the nuclear matrix in spermatids of an organism that shows lamellar-mediated chromatin condensation. A possible candidate for such chromatin/nucleoplasm patterning is the internally fertilizing grasshopper *Pyrgomorpha conica* [97], as several other related orthopteran showing such patterning have already been listed in (Table (**I**)). This organism has chromatin scaffolds in the central spermatid core. According to Cerna, *et al.* [[97], p.22]: "The expanded DNA loops when anchored through triplex DNA motifs to the scaffold will endure important changes, including the formation of DNA breaks, sequential replacement of their histones by transition proteins and protamines, and, overall, the extreme chromatin condensation and packing achieved by late spermiogenesis."

A polar nuclear matrix has been observed in spermatids of the internally fertilizing *Octopus vulgaris* [98], but only a pattern of parallel fibers forms in the condensing nucleus during spermiogenesis; no lamellae are found.

Third, steps B, C, D in the patterning stage of *S. canicula* spermiogenesis in (Fig. (**3**), as magnified in (Fig. (**4**)), appear to show a constancy of spacing from the middle of one lamella to the middle of an adjacent one, as diagrammed in (Fig. (**5**, left.)) This is λ, the unit of pattern that, according to Cahn's [81] thermodynamic analysis of spinodal decomposition, shows a maximal value when plotted against a growth rate constant [[79], Fig. **8**]. In other words, according to Jones [[93], p.33, in legend to Fig. **3.7**] for sinusoidal distributions of concentration, "…concentraton fluctuations of one particular intermediate length scale grow fastest in spinodal decomposition".

In order to visualize this more readily, one of us (H.E.K.) has measured λ in every panel in (Fig. (**4**)) using a finely calibrated Staedtler steel ruler. In (Fig. (5, left column)), we can readily see from the histograms that λ_m for *S. canicula* spermiogenesis (shaded bars) is constant for steps A-D (35-40 nm, 30-35 nm, 30-35 nm, 30-35 nm) during the patterning stage, then diminishes to 10-15 nm in step E (measured from [[86], Fig. **26**, 240,000X] during the condensation stage, and to homogeneity in the late spermatid nucleus in step F. Values at each step in spermiogenesis for λ, pattern repeat distance; d, diameter of chromatin; w, width of nucleoplasm; n.d., diameter of nucleus, are indicated in Fig. (**3**, left)). Most interestingly, Livolant *et al*. [[99], p.2629] note the following: "Lamellar structures with a periodicity of about 50 nm were also described in the fish *Scyliorhinus* sperm cell at a given step of the spermiogenesis process (Gusse and Chevaillier 1978)" [86].

The histograms of the 40/60 PDLC (Fig. 5, center column) also show relatively constant values for λ_m for the optical photomicrographs of (Fig. **4,** center column) from 3 minutes to 120 minutes (2.5-3 μm, 2.5-3 μm, 3.5-4 μm, 3.5-4 μm). After this time, heterogeneous droplets begin to appear at 300 minutes and particularly at 1020 minutes in (Fig. (**5,** center column)), yielding "twin towers" (3.5-4 μm and 4.5-5 μm), and then a very dispersed histogram (3-13.5 μm). This final step is even more dispersed than the final step of the nucleation and growth (1.5-7 μm). Interestingly, the distances between the centers of droplets are also relatively constant (1.5-4 μm) for nucleation and growth (Fig. (**5**, right column)).

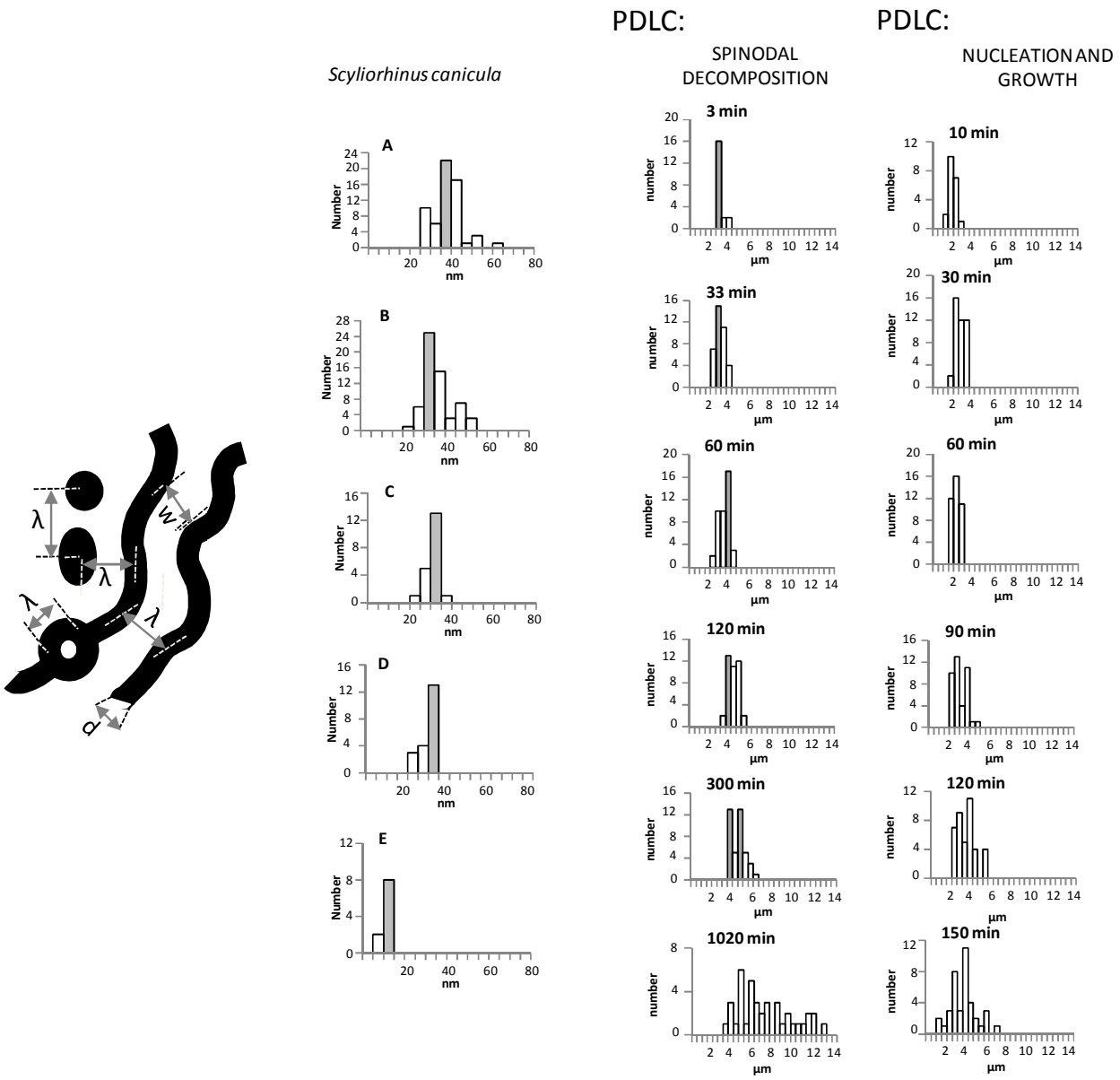

Figure 5. Histograms of the pattern repeat distance (λ) for spermatid nuclei in TEM photomicrographs of the dogfish *S. canicula* and polarized optical photomicrographs of PDLC. Features are indicated in the diagram (on the left) for which λ (lambda, a unit of pattern) can be measured during spermiogenesis from the middle of the black chromatin stripe, dot or doughnut-like formation, across the white nucleoplasm, to another formation of chromatin in (Fig. (**4**)), along with the diameter (d) of the chromatin fiber, the width (w) of the nucleoplasm and the diameter of the nucleus (n.d.). λ can also be measured during the time evolution of a PDLC undergoing either spinodal decomposition or nucleation and growth. The shaded bar in each histogram represents λ_m (lambda maximum, the dominant pattern repeat distance). All measured values for λ_m, along with d, w and n.d., for spermiogenesis in *S. canicula* are summarized in (Fig. (**3**)) to the left of each TEM photomicrograph.

DIVERSITY OF SPECIES SHOWING CHROMATIN/ NUCLEOPLASM PATTERNING DURING SPERMIOGENESIS

Table (**I**) lists several dozen species with chromatin/nucleoplasmic patterning, showing that a lamellar step in mid-spermiogenesis is widespread in evolution. However, this only occurs during spermiogenesis in a small minority of internally fertilizing species in animals, as well as in several species of algae that show features similar to internal fertilization in animals. Analysis of the histone-to-protamine transition and possible processing or modification of protamines for these organisms is mostly limited to those discussed in this and previous papers [20, 79]. Chromatin/nucleoplasm inversion may be the case in both an octopus and a relict ciliate.

Why is there so much diversity in the type of species and such a low number of species that display patterning of

Table I. Internally Fertilizing Organisms Showing Chromatin/Nucleoplasm Lamellar Patterning (or Inversion) During Spermiogenesis. (1; See Footnotes at Bottom of Table)

Species	Reference	Description
VERTEBRATES		
CARTILAGINOUS FISH:		
Scyliorhinus canicula	[86]	Dogfish. See (Fig. (2-4)). Marine.
Squalus suckleyi	[101, 102]	Spiny dogfish. Similar to *S. canicula*.
Himantura signifer	[100]	Stingray. Fresh water. Similar to *S. canicula*.
Hydrolagus colliei [103]	Ratfish	
INVERTEBRATES		
MOLLUSCS:		
MESOGASTROPODS:		
Littorina sitkana	[126]	Periwinkle. Marine snail.
Viviparus contectoides	[127]	Prosobranch. Fresh water.
NEOGASTROPODS:		
Murex brandaris	[79]	Muricid snail. Marine.
Nucella lamellosa	[20]	Muricid snail. Similar to *M. brandaris*.
Nucella lapillus	[122]	Muricid snail. Similar to *M. brandaris*.
Nucella crassilabrum	[123]	Muricid snail. Similar to *M. brandaris*.
Chorus giganteus	[124]	Muricid snail. Similar to *M. brandaris*.
Thais hemostoma	[125]	Muricid snail.
PULMONATES:		
Helix aspersa	[118]	Land snail.
Otala lactea	[128]	Land snail.
CEPHALOPODS:		
Eledone cirrhosa	[79]	Octopus. (2)
Arthropods:		
INSECTS:		
Philaenus spumarius	[79]	Spittlebug. Homopteran.
Tylozygres sp.	[111]	Leafhopper. Hemipteran.
Euchistus heros	[129]	Phytophagous bug. Hemipteran.
Triatoma infestans	[119]	Cone-nose bug. Hemipteran.
Acheta domestica	[113, 114]	House cricket. Orthopteran.
Gryllis pennsylvanicus	[114]	Field cricket. Orthopteran.
Melanoplus sp.	[111]	Grasshopper. Orthopteran.
Locusta migratoria	[130]	Locust, Orthopteran.
Blatella germanica	[131]	Cockroach. Blattodean.
Laccotrephes sp.	[132]	Heteropteran.
Gerris najas	[133]	Waterstrider. Heteropteran.

(Table 1) Contd….

Species	Reference	Description
Leptogaster sp.	[111]	Robber fly. Dipteran.
Bacillus rossius	[134]	Stick insect. Phasmatodean.
Potamophylax		
rotundipennis	[135]	Caddis fly. Trichopteran.
Thermobia domestica	[136]	Fire-brat insect. Thysanuran.
PLATYHELMINTHS:		
Phaenocora anomalocoela	[137]	Turbellarian. Flatworm.
ACANTHOCEPHALANS:		
Macracanthorhynchus		
hirudinaceus	[138]	Parasite acanthocephalan of wild boar.
ALGAE		
Chara (fibrosa)	[139]	Multicellular green alga. Stonewort. (3)
Chara vulgaris	[140]	Multicellular green alga. Stonewort. (3)
PROTISTS		
Trachelocerca multinucleata	[141]	Karyorelectid ciliate. (4)

(1) TEM photomicrographs were examined (from the published literature) of testis fixed in glutaraldehyde and stained with metals, except for testis subjected to high-pressure freezing in *Nucella lamellosa*.
(2) After lamellae formation [36], the spermatid nucleus undergoes an inversion from chromatin in nucleoplasm to nucleoplasm in chromatin.
(3) A biflagellated sperm fertilizes the egg in freshwater after penetrating "the narrow fissure between the coronula cells and the upper ends of the cortical filaments…."[[142], Fig. **30.3** and p. 480].
(4) Nucleoplasm in spongy chromatin of a micronucleus; possibly an inversion. [[141], Fig. **2c**]. Haploid nuclei, derived from micronuclei, are mutually exchanged during conjugation (fusion of conspecific cells) [[143], Fig. **263**].

spermiogenic chromatin/nucleoplasm? We speculate that the species in (Table (**I**)) displaying phase separation by spinodal decomposition during spermiogenesis are just a small subset of internally fertilizing species that happen to have the appropriate biochemistry in their histone-to-protamine transition to fall into the unstable portion of the phase diagram (Fig. (**4**, left)).

For example, amongst the internally fertilizing chondrichthyan fish (Table (**I**)), we have already seen (Fig. (**4**)) that the spermatid of the elasmobranch dogfish *S. canicula* displays the bicontinuous lamellar chromatin/nucleoplasm patterning typical of phase separation by spinodal decomposition, while undergoing a transition from histones to intermediate proteins to protamine and keratinous protamines (Fig. (**3**)). The spermatid of the elasmobranch stingray *Himantura signifer* [100] also shows such patterning, as does the spiny dogfish *Squalus suckleyi* [101, 102], but no biochemical analyses have been reported. In the spermatid nucleus of the holocephalon ratfish *Hydrolagus colliei*, Stanley *et al.* [[103], Fig. **1**, stage 6] find "distinct chromatin fibers longitudinally oriented but bound side by side into anastomosing sheets." This is also suggestive of a bicontinuous lamellar-mediated chromatin condensation. In *H. colliei* there is a transition from histones to protamines and keratinous protamines [104]. However, the latter proteins do not contain as many cysteine residues as in *S. canicula* spermatids, perhaps limiting the extent of disulfide bond formation in *H. colliei*.

It would be interesting, therefore, to compare this situation in cartilaginous fish with possible chromation patterning and the histone to protamine transition in bony fish that also have internal fertilization. The spermatid of the viviparous brotula *Cataetyx laticeps* (Bythitidae) undergoes a transition from histone to a H5-like histone during spermiogenesis [105], whereas the rockfish *Sebastes maliger* (Scorpaenidae) [68] undergoes a histone to protamine transition. No keratinous protamines are found. Chromatin structural changes in the nucleus during spermiogenesis have not been analyzed in these bony fish.

However, in *Helicolenus dactylopterus dactylopterus* (Scorpaenidae), an internally fertilizing bony fish closely related to *S. maliger*, a lower resolution TEM micrograph [[106], Fig. **2E**] indicates the possibility that some features of lamellar-like chromatin/nucleopasm patterning might be present in spermatids during mid-spermiogenesis. If this observation can be validated by higher resolution TEM analysis of the entire spermiogenic developmental profile, it would suggest that either the histone-to-protamine transition, or the histone-to-keratinous protamine transition, could provide the phase conditions that place the spermatid nucleus of internally fertilizing fish into the unstable region of the $1/\chi$ - C phase diagram.

Other internally fertilizing species, including mammalian ones, likely happen to fall into the metastable portion of this phase diagram and therefore display nucleation and growth.

The externally fertilizing species look more like phase separation by nucleation and growth as they generally retain the granular chromatin condition and their sperm nuclear basic proteins (SNBPs) are "simple" protamines or protamine-like compared to the more "complex" protamines of internally fertilizing species resulting from replacement (Fig. (**1**, right, middle)), processing (Fig. (**1**, right, bottom)), and side chain modification (Fig. (**3**, right)).

However, even here small differences in the sequence of "simple" protamines makes spermiogenesis in the externally fertilizing bony fish *Dicentrarchus labrax* [[55], Fig. **5**] look more like nucleation and growth (Fig. (**4**, right column)), while externally fertilizing rainbow trout (*Salmo gairdneri*) [[107], Fig. **18**] is more complex than that, developing from coarse granules into thick fibers. However, both species definitely lack the bicontinuous lamellae characteristic of spinodal decomposition (Fig. (**4**, left and center columns)).

All of these findings, taken together, suggest that phase separation by either mechanism may play an important role in chromatin remodelling during spermiogenesis. The transient patterning that accompanies phase separation by spinodal decomposition enables us to understand what is happening in TEM photomicrographs, but only for a small minority of species that show the complete transition from granules to fibers to lamellae.

For example, while a few species of internally fertilizing molluscs, insects and cartilaginous fish display features of spinodal decomposition during spermiogenesis (Table (**I**)), many more species of internally fertilizing mammals [108], as well as externally fertilizing bony fish, display features of nucleation and growth of chromatin granules during spermiogenesis. In mammalian species chromatin forms 60-100 nm toroids [1, 56, 109] rather than bicontinuous patterns. While a complete explanation for this is not as yet available, there are several considerations worth noting.

First, spinodal decomposition **(**Fig. (**4,** left and center columns)), and nucleation and growth **(**Fig. (**4,** right column)) may represent the extremes of a single mechanism of phase separation rather than separate processes. As Gunton *et al*. [[110], p.364] point out: "Thus in the classical pictures of nucleation and of spinodal decomposition, there is a sharp transition between metastable and unstable states as characterized by the classical spinodal curve". However, since Cahn [81] proposed his classical theory of spinodal decomposition, more recent theoretical analysis suggests that "spinodal decomposition could be viewed as a generalized nucleation. Thus the long wavelength fluctuations which characterize spinodal decomposition can be considered as an extreme version of nucleation, involving a very low activation energy" [[110], p.366].

In addition, there appears to be boundary conditions in a spermatid nucleus at the nuclear envelope and, in some species, at the membrane bounding the axoneme. These boundary conditions may be forcing chromatin to orient either perpendicular to the nuclear envelope when an axoneme is present and parallel with the nuclear envelope when it is not. This is in order to obtain the configuration of lowest energy in spinodal decomposition, where no (classically) or little activation energy is needed. Nucleation and growth do have to overcome an initial energy barrier in any event.

In other words, can the axoneme, which develops into the nucleus in the head of the sperm, be regarded as a "patch"; i.e., as a discrete region that is distinguished from the major volume of chromatin condensing in the nucleoplasm? Perhaps the membrane bounding the axoneme is providing a diffusion barrier. This may also be the case for the "patches" of granular chromatin in several regions near the nuclear envelope, as seen in TEM photomicrographs of transverse sections [[85], Fig. **2-8**] in the homopteran insect (Table (**I**) *Philaenus spumarius* [[79], Fig. **1**] and in other insects [[111], Fig. **41**, **42**]. This results in chromatin/nucleoplasm patterning occurring in the bulk of the interior of the nucleus, but less so at the periphery.

Also, spermatids of other organisms employing nucleation and growth, such as the mouse, may have a "patch." In this case, chromatin arises centrifugally from that core "patch" during spermiogenesis [112].

What is the temporal relation between the histone-to-protamine transition and patch-generating condensed chromatin? In house cricket [113, 114] there appears to be two rounds of spinodal decomposition, as manifested by the development of lamellae, We suggest that the first region of condensed chromatin may act as a "patch" for the second round.

Secondly, it is not clear as yet whether it is microemulsification [115], as suggested by Harrison *et al*. [79], electrostatics [116, 117], or some combination of these that is capable of slowing down the process of spermiogenesis sufficiently so that a patterning stage is apparent in the TEM photomicrographs of spermatids for species showing spinodal decomposition. For example, with respect to the timing of lamellae formation during spermiogenesis, we know that in the pulmonate snail *Helix aspersa*, [118], lamellar steps take 3.8 /22.7 days, or only 17% of the total duration of spermiogenesis, and also "occur very rapidly" [[119], p.288] in the hemipteran insect *Triatoma infestans*.

Thirdly, with respect to DNA condensation by multivalent cations, Bloomfield [[120], p.273] asks: "Why Toroids?.... Given that solvent conditions are sufficient to cause collapse of the extended DNA chain, why are toroids formed, rather than spherical globules, or rods, or lamellae?... Most of the answer lies in the stiffness of DNA, the rather weak attractive forces between DNA segments, and the very low DNA concentrations at which condensation experiments are generally done".

In fact, we have seen (Table (**I**)) that lamellae can be formed in spermatids of several dozen internally fertilizing diverse species, Therefore, we put forward the hypothesis that lamellar chromatin/nucleoplasm patterning during spermiogenesis may be the visual manifestation of the mechanism of liquid-liquid phase separation by spinodal decomposition when the appropriate concentrations of complex protamines and DNA fall into the unstable region of the phase diagram (Fig. (**4.** left)). This occurs during histone-to-protamine replacement, and SNBP processing and side chain modification of spermiogenic chromatin. Such an hypothesis complements our present knowledge of phase separation in

the metastable portion of the phase diagram by nucleation and growth during mammalian spermiogenesis [109].

What is needed now is to verify this hypothesis experimentally. Bertin *et al*. [[121], Fig. **8**] and Livolant *et al*. [[99], Fig. **3**] have obtained experimental phase diagrams for nucleosome core particles aggregated by multivalent cations (spermidine) or monovalent cations (sodium), respectively. This is probably the highest order of chromatin structure examined so far. Chromatin during the patterning stage of spermiogenesis that is subjected to spinodal decomposition in the unstable region of a phase diagram is as yet too complex and dynamic to be analyzed successfully in this manner. However, it is certainly worthwhile to continue to explore this experimentally. As Livolant *et al.* [[99], p. 2629] declare, in the living cell, such complexity "…may offer extremely high possibilities of adaptation of chromatin organization to multiple local restraints".

ACKNOWLEDGEMENTS

We are very grateful to Lindsay Frehlick, Garnet Martens, Ron Fin and Anita Thambirajah for assistance in the preparation of Figs. **3**, **4** and **5**. This work was supported by a grant from the Natural Sciences and Engineering Research Council of Canada [NSERC-OGP-0046399-02] (to J.A.) and by a contract from the Ramon y Cajal Subprogramme from the Spanish Government-MICINN and by a Research Grant from the Xunta de Galicia (10-PXIB-103-077-PR) (to J.M.E.-L.).

REFERENCES

[1] Balhorn, R. The protamine family of sperm nuclear proteins. *Genome Biol.*, **2007**, *8*, 227.

[2] Ausió, J. Histone H1 and evolution of sperm nuclear basic proteins. *J. Biol. Chem.*, **1999**, *274*, 31115-31118.

[3] Eirín-López, J.M.; Ausió, J. Origin and evolution of chromosomal sperm proteins. *Bioessays*, **2009**, *31*, 1062-1070.

[4] Lewis, J.D.; Song, Y.; de Jong, M.; Bagha, S.; Ausió, J. A walk though vertebrate and invertebrate protamines. *Chromosoma*, **2003**, *111*, 473-482.

[5] Eirín-López, J.M.; Lewis, J.D.; Howe, L.; Ausió, J. Common phylogenetic origin of protamine-like (PL) proteins and histone H1: evidence from bivalve PL genes. *Mol. Biol. Evol.*, **2006**, *23*, 1304-1317.

[6] Hunt, J.G.; Kasinsky, H.E.; Elsey, R.M.; Wright, C.L.; Rice, P., *et al*. Protamines of reptiles. *J. Biol. Chem.*, **1996**, *271*, 23547-23557.

[7] Luger, K.; Mäder, A.W.; Richmond, R.K.; Sargent, D.F.; Richmond, T.J. Crystal structure of the nucleosome core particle at 2.8 A resolution. *Nature*, **1997**, *389*, 251-260.

[8] McGhee, J.D.; Felsenfeld, G. The number of charge-charge interactions stabilizing the ends of nucleosome DNA. *Nucleic Acids Res.*, **1980**, *8*, 275127-275169.

[9] van Holde, K.E. *Chromatin*, Springer-Verlag: New York, NY, **1988**.

[10] Raukas, E.; Mikelsaar, R.H. Are there molecules of nucleoprotamine? *Bioessays*, **1999**, *21*, 440-448.

[11] Gaucher, J.; Reynoird, N.; Montellier, E.; Boussouar, F.; Rousseaux, S., *et al*. From meiosis to postmeiotic events: the secrets of histone disappearance. *FEBS J.*, **2010**, *277*, 599-604.

[12] Churikov, D.; Siino, J.; Svetlova, M.; Zhang, K.; Gineitis, A., *et al*. Novel human testis-specific histone H2B encoded by the interrupted gene on the X chromosome. *Genomics*, **2004**, *84*, 745-756.

[13] Govin, J.; Escoffier, E.; Rousseaux, S.; Kuhn, L.; Ferro, M., *et al*. Pericentric heterochromatin reprogramming by new histone variants during mouse spermiogenesis. *J. Cell Biol.*, **2007**, *176*, 283-294.

[14] Ishibashi, T.; Li, A.; Eirín-López, J.M.; Zhao, M.; Missiaen, K., *et al*. H2A.Bbd: An X-chromosome-encoded histone involved in mammalian spermiogenesis. *Nucleic Acids Res.*, **2010**, *38*, 1780-1789.

[15] Lewis, J.D.; Abbott, D.W.; Ausió, J. A haploid affair: core histone transitions during spermatogenesis. *Biochem. Cell Biol.*, **2003**, *81*, 131-140.

[16] Oliva, R.; Dixon, G.H. Vertebrate protamine genes and the histone-to-protamine replacement reaction. *Prog. Nucleic Acid Res. Mol. Biol.*, **1991**, *40*, 25-94.

[17] Awe, S.; Renkawitz-Pohl, R. Histone H4 acetylation is essential to proceed from a histone- to a protamine-based chromatin structure in spermatid nuclei of Drosophila melanogaster. *Syst. Biol. Reprod. Med.*, **2010**, *56*, 44-61.

[18] Baarends, W.M.; Hoogerbrugge, J.W.; Roest, H.P.; Ooms, M.; Vreeburg, J., *et al*. Histone ubiquitination and chromatin remodeling in mouse spermatogenesis. *Dev. Biol.*, **1999**, *207*, 322-333.

[19] Lu, L.Y.; Wu, J.; Ye, L.; Gavrilina, G.B.; Saunders, T.L., *et al*. RNF8-dependent histone modifications regulate nucleosome removal during spermatogenesis. *Dev. Cell*, **2010**, *18*, 371-384.

[20] Martens, G.; Humphrey, E.C.; Harrison, L.G.; Silva-Moreno, B.; Ausió, J., *et al*. High-pressure freezing of spermiogenic nuclei supports a dynamic chromatin model for the histone-to-protamine transition. *J. Cell. Biochem.*, **2009**, *108*, 1399-1409.

[21] Kasinsky, H.E. In: *Histones and Other Basic Nuclear Proteins* Hnilica, L.S.; Stein, G.S.; Stein, J.L., Eds.; CRC Press: Boca Raton, FL, **1989**; pp. 73-163.

[22] Kasinsky, H.E. In: *Advances in Spermatozoal Phylogeny and Taxonomy*; Jamieson, B.G.M.; Ausió, J.; Justine, J.L., Eds.; Memoires de Museum National d'Histoire Naturelle: Paris, France, **1995**; pp. 447-462.

[23] Subirana, J.A. In: *Proceedings of the Fourth International Symposium on Spermatology*; André, J., Ed Maltinus Nijhoff: The Hague, **1983**; pp. 197-213.

[24] Ausió, J.; Greulich, K.O.; Haas, E.; Wachtel, E. Characterization of the fluorescence of the protamine thynnine and studies of binding to double-stranded DNA. *Biopolymers*, **1984**, *23*, 2559-2571.

[25] Helene, C.; Lancelot, G. Interactions between functional groups in protein-nucleic acid associations. *Prog. Biophys. Mol. Biol.*, **1982**, *39*, 1-68.

[26] Puigdomenech, P.; Martínez, P.; Palau, J.; Bradbury, E.M.; Crane-Robinson, C. Studies on the role and mode of operation of the very-lysine-rich histones in eukaryote chromatin. Nuclear-magnetic-resonance studies on nucleoprotein and histone phi 1-DNA complexes from marine invertebrate sperm. *Eur. J. Biochem.*, **1976**, *65*, 357-363.

[27] Steger, K. Haploid spermatids exhibit translationally repressed mRNAs. *Anat. Embryol.*, **2001**, *203*, 323-334.

[28] Barreau, C.; Benson, E.; Gudmannsdottir, E.; Newton, F.; White-Cooper, H. Post-meiotic transcription in Drosophila testes. *Development*, **2008**, *135*, 1897-1902.

[29] Chalmel, F.; Rolland, A.D.; Niederhauser-Wiederkehr, C.; Chung, S.S.; Demougin, P., *et al.* The conserved transcriptome in human and rodent male gametogenesis. *Proc. Natl. Acad. Sci. U S A*, **2007**, *104*, 8346-8351.

[30] Schulz, R.W.; de Franca, L.R.; Lareyre, J.J.; Legac, F.; Chiarini-Garcia, H., *et al.* Spermatogenesis in fish. *Gen. Comp. Endocrinol.*, **2009**, *163*, 329-339.

[31] Vibranowsky, M.D.; Lopes, H.F.; Karr, T.L.; Long, M. Stage-specific expression profiling of Drosophila spermatogenesis suggests that meiotic sex chromosome inactivation drives genomic relocation of testis-expressed genes. *PLoS Genet.*, **2009**, *5*, e1000731.

[32] Ausió, J.; Brewer, L.R.; Frehlick, L.J. In: *Epigenetics and Reproduction*; Rousseaux, S.; Khochbin, S., Eds.; Springer-Verlag: **2010**; pp.

[33] Verdaguer, N.; Perello, M.; Palau, J.; Subirana, J.A. Helical structure of basic proteins from spermatozoa. Comparison with model peptides. *Eur. J. Biochem.*, **1993**, *214*, 879-887.

[34] Dunker, A.K.; Lawson, J.D.; Brown, C.J.; Williams, R.M.; Romero, P., *et al.* Intrinsically disordered protein. *J. Mol. Graph. Model.*, **2001**, *19*, 26-59.

[35] Hansen, J.C.; Lu, X.; Ross, E.D.; Woody, R.W. Intrinsic protein disorder, amino acid composition, and histone terminal domains. *J. Biol. Chem.*, **2006**, *281*, 1853-1856.

[36] Gimenez-Bonafe, P.; Ribes, E.; Sautiere, P.; González, A.; Kasinsky, H.E., *et al*. Chromatin condensation, cysteine-rich protamine, and establishment of disulphide interprotamine bonds during spermiogenesis of *Eledone cirrhosa* (Cephalopoda). *Eur. J. Cell Biol.*, **2002**, *81*, 341-349.

[37] Jayaramaiah Raja, S.; Renkawitz-Pohl, R. Replacement by Drosophila melanogaster protamines and Mst77F of histones during chromatin condensation in late spermatids and role of sesame in the removal of these proteins from the male pronucleus. *Mol. Cell. Biol.*, **2005**, *25*, 6165-6177.

[38] Ausió, J.; Eirín-López, J.M.; Frehlick, L.J. In: *Spermatology*; Roldan, E.R.S.; Gomendio, M., Eds.; Nottingham University Press: Nottingham, **2007**; pp. 63-79.

[39] Ausió, J.; Saperas, N.; Chiva, M. In: *Cryopreservation in Aquatic Species, 2nd edition*; Tiersch, T.; Green, C., Eds.; World Aquaculture Society: Baton Rouge, Louisiana, **2009**; pp.

[40] Saowaros, W.; Panyim, S. The formation of disulfide bonds in human protamines during sperm maturation. *Experientia*, **1979**, *35*, 191-192.

[41] Vilfan, I.D.; Conwell, C.C.; Hud, N.V. Formation of native-like mammalian sperm cell chromatin with folded bull protamine. *J. Biol. Chem.*, **2004**, *279*, 20088-20095.

[42] Björndahl, L.; Kvist, U. Human sperm chromatin stabilization: a proposed model including zinc bridges. *Mol. Hum. Reprod.*, **2009**, *16*, 23-29.

[43] Bianchi, F.; Rousseaux-Prevost, R.; Sautiere, P.; Rousseaux, J. P2 protamines from human sperm are zinc -finger proteins with one CYS2/HIS2 motif. *Biochem. Biophys. Res. Commun.*, **1992**, *182*, 540-547.

[44] Gatewood, J.M.; Schroth, G.P.; Schmid, C.W.; Bradbury, E.M. Zinc-induced secondary structure transitions in human sperm protamines. *J. Biol. Chem.*, **1990**, *265*, 20667-20672.

[45] Hecht, N.B. In: *Histones and Other Basic Nuclear Proteins*; Hnilica, L.S., Ed CRC Press: Boca Raton, Florida, **1989**; pp. 347-373.

[46] Gimenez-Bonafe, P.; Laszczak, M.; Kasinsky, H.E.; Lemke, M.J.; Lewis, J.D., *et al*. Characterization and evolutionary relevance of the sperm nuclear basic proteins from stickleback fish. *Mol. Reprod. Dev.*, **2000**, *57*, 185-193.

[47] Retief, J.D.; Winkfein, R.J.; Dixon, G.H.; Adroer, R.; Queralt, R., *et al*. Evolution of protamine P1 genes in primates. *J. Mol. Evol.*, **1993**, *37*, 426-434.

[48] Wyckoff, G.J.; Wang, W.; Wu, C.I. Rapid evolution of male reproductive genes in the descent of man. *Nature*, **2000**, *403*, 304-309.

[49] Swanson, W.J.; Vacquier, V.D. The rapid evolution of reproductive proteins. *Nat. Rev. Genet.*, **2002**, *3*, 137-144.

[50] Rolland, A.D.; Lareyre, J.J.; Goupil, A.S.; Montfort, J.; Ricordel, M.J., *et al*. Expression profiling of rainbow trout testis development identifies evolutionary conserved genes involved in spermatogenesis. *BMC Genomics*, **2009**, *10*, 546.

[51] Morinière, J.; Rousseaux, S.; Steuerwald, U.; Soler-López, M.; Curtet, S., *et al*. Cooperative binding of two acetylation marks on a histone tail by a single bromodomain. *Nature*, **2009**, *461*, 664-668.

[52] Kee, K.; Angeles, V.T.; Flores, M.; Nguyen, H.N.; Reijo Pera, R.A. Human DAZL, DAZ and BOULE genes modulate primordial germ-cell and haploid gamete formation. *Nature*, **2009**, *462*, 222-225.

[53] Oliva, R. Protamines and male infertility. *Hum. Reprod. Update*, **2006**, *12*, 417-435.

[54] Rhim, J.A.; Connor, W.; Dixon, G.H.; Harendza, C.J.; Evenson, D.P., *et al*. Expression of an avian protamine in transgenic mice disrupts chromatin structure in spermatozoa. *Biol. Reprod.*, **1995**, *52*, 20-32.

[55] Saperas, N.; Ribes, E.; Buesa, C.; Garcia-Hegart, F.; Chiva, M. Differences in chromatin condensation during spermiogenesis in two species of fish with distinct protamines. *J. Exp. Zool.*, **1993**, *265*, 185-194.

[56] Balhorn, R.; Cosman, M.; Thornton, K.; Krishnan, V.V.; Corzett, M., *et al*. In: *The Male Gamete: From Basic To Clinical Applications*; Gagnon, C., Ed Cache River Press: Vienna, Illinois, **1999**; pp. 58-70.

[57] Ohta, T. On the evolution of multigene families. *Theor. Popul. Biol.*, **1983**, *23*, 216-240.

[58] Ausió, J. Histone variants: the structure behind the function. *Brief. Funct. Genomic. Proteomic.*, **2006**, *5*, 228-243.

[59] Eirín-López, J.M.; González-Romero, R.; Dryhurst, D.; Méndez, J.; Ausió, J. In: *Evolutionary Biology: Concept, Modeling, and Application*; Pontarotti, P., Ed Springer-Verlag: Berlin Heidelberg, **2009**; pp. 139-162.

[60] Nei, M.; Rooney, A.P. Concerted and birth-and-death evolution in multigene families. *Annu. Rev. Genet.*, **2006**, *39*, 121-152.

[61] Malik, H.S.; Henikoff, S. Phylogenomics of the nucleosome. *Nat. Struct. Biol.*, **2003**, *10*, 882-891.

[62] Eirín-López, J.M.; González-Tizón, A.M.; Martínez, A.; Méndez, J. Birth-and-death evolution with strong purifying selection in the histone H1 multigene family and the origin of orphon H1 genes. *Mol. Biol. Evol.*, **2004**, *21*, 1992-2003.

[63] Eirín-López, J.M.; Frehlick, L.J.; Ausió, J. Protamines, in the footsteps of linker histone evolution. *J. Biol. Chem.*, **2006**, *281*, 1-4.

[64] Bloch, D.P. In: *Handbook of Genetics*; King, R.C., Ed Plenum Press: New York, **1976**; pp. 139-167.

[65] Eirín-López, J.M.; González-Tizón, A.M.; Martínez, A.; Méndez, J. Molecular and evolutionary analysis of mussel histone genes (Mytilus spp.): possible evidence of an "orphon origin" for H1 histone genes. *J. Mol. Evol.*, **2002**, *55*, 272-283.

[66] Eirín-López, J.M.; Frehlick, L.J.; Chiva, M.; Saperas, N.; Ausió, J. The sperm proteins from amphioxus mirror its basal position among chordates and redefine the origin of vertebrate protamines. *Mol. Biol. Evol.*, **2008**, *25*, 1705-1713.

[67] Lewis, J.D.; Saperas, N.; Song, Y.; Zamora, M.J.; Chiva, M., *et al*. Histone H1 and the origin of protamines. *Proc. Natl. Acad. Sci. U S A*, **2004**, *101*, 4148-4152.

[68] Frehlick, L.J.; Eirín-López, J.M.; Prado, A.; Su, H.W.; Kasinsky, H.E., *et al*. Sperm nuclear basic proteins of two closely related species of Scorpaeniform fish (Sebastes maliger, Sebastolobus sp.) with different sexual reproduction and the evolution of fish protamines. *J. Exp. Zoolog. A Comp. Exp. Biol.*, **2006**, *305*, 277-287.

[69] Rooney, A.P.; Zhang, J.; Nei, M. An unusual form of purifying selection in a sperm protein. *Mol. Biol. Evol.*, **2000**, *17*, 278-283.

[70] Ausió, J.; Soley, J.T.; Burguer, W.; Lewis, J.D.; Barreda, D., *et al*. The histidine-rich protamine from ostrich and tinamou sperm. A link between reptile and bird protamines. *Biochemistry*, **1999**, *38*, 180-084.

[71] Queralt, R.; Adroer, R.; Oliva, R.; Winkfein, R.J.; Retief, J.D., *et al*. Evolution of protamine P1 genes in mammals. *J. Mol. Evol.*, **1995**, *40*, 601-607.

[72] Retief, J.D.; Dixon, G.H. Evolution of pro-protamine P2 genes in primates. *Eur. J. Biochem.*, **1993**, *218*, 1095.

[73] Saperas, N.; Buesa, C.; Abian, J.; Vanderkerckhove, J.; Kasinsky, H.E., *et al*. The primary structure of a chondrichthyan protamine: a new apparent contradiction in protamine evolution. *J. Mol. Evol.*, **1996**, *43*, 528-535.

[74] Krawetz, S.A.; Dixon, G.H. Sequence similarities of the protamine genes: implications for regulation and evolution. *J. Mol. Evol.*, **1988**, *27*, 291-297.

[75] Retief, J.D.; Krajewski, C.; Westerman, M.; Dixon, G.H. The evolution of protamine P1 genes in dasyurid marsupials. *J. Mol. Evol.*, **1995**, *41*, 549-555.

[76] Cáceres, C., L.; Giménez-Bonafé, P.; Ribes, E.; Wouters-Tyrou, D.; Martinage, A., *et al*. DNA-interacting proteins in the spermiogenesis of the mollusc Murex brandaris. *J. Biol. Chem.*, **1999**, *274*, 649-656.

[77] Cáceres, C.; Gimenez-Bonafe, P.; Zamora, M.J.; Ribes, E.; Saperas, N., *et al*. Protamines in archaeogastropod and cenogastropod molluscs: An example of a radical evolutionary change in a protein model. *Trends Comp. Biochem. Physiol.*, **2000**, *7*, 75-82.

[78] Cáceres, C.; Ribes, E.; Muller, S.; Cornudella, L.; Chiva, M. Characterization of chromatin-condensing proteins during spermiogenesis in a neogastropod mollusk (Murex brandaris). Mol. Reprod. Dev., 1994, 38, 440-452. *Mol. Reprod. Dev.*, **1994**, *38*, 440-452.

[79] Harrison, L.G.; Kasinsky, H.E.; Ribes, E.; Chiva, M. Possible mechanisms for early and intermediate stages of sperm chromatin condensation patterning involving phase separation dynamics. *J. Exp. Zool. A Comp. Exp. Biol.*, **2005**, *303*, 76-92.

[80] Turing, A.M. The chemical basis of morphogenesis *Phil. Trans. R. Soc. Lond. B*, **1952**, *237*, 37-72.

[81] Cahn, J.W. Phase separation by spinodal decomposition in isotropic systems. *J. Chem. Phys.*, **1965**, *42*, 93-99.
[82] Gunton, J.D.; Droz, M. *Introduction to the Theory of Metastable and Unstable States*, Springer-Verlag: Berlin, **1983**.
[83] Jantzen, C.M.F.; Herman, H. In: *Phase Diagrams: Materials Science and Technology*; Alper, A.M., Ed Academic Press: New York, USA, **1978**; pp. 127-184.
[84] Raspaud, E.; Olivera de la Cruz, M.; Sikorav, J.-L.; Livolant, F. Precipitation of DNA by polyamines: a polyelectrolyte behavior. *Biophys. J.*, **1998**, *74*, 381-393.
[85] Chevaillier, P. In: *Comparative Spermatology*; Baccetti, B., Ed Academic Press: New York, USA, **1969**; pp. 499-514.
[86] Gusse, M.; Chevaillier, P. Étude ultrastructurale et chimique de la chromatine au cours de la spermiogenèse de la roussette Scylliorhinus caniculus (L.). *Cytobiologie*, **1978**, *16*, 421-443.
[87] Compagno, L.J.V. In: *Reproductive Biology and Phylogeny of Chondrichthyes: Sharks, Batoids and Chimaeras*; Hamlett, W.C.; Jamieson, B.G.M., Eds.; Science Publishers: Enfield, New Hampshire, USA, **2005**; pp. 503-548.
[88] Chevaillier, P. In: *Comparative Spermatology: 20 Years After*; Baccetti, B., Ed Raven Press: New York, USA, **1991**; pp. 19-25.
[89] Gusse, M.; Chevaillier, P. Microelectrophoretic analysis of basic protein changes during spermiogenesis in the dogfish Scylliorhinus caniculus (L.). *Exp. Cell Res.*, **1981**, *136*, 391-397.
[90] Kouach, M.; Jaquinod, M.; Belaiche, D.; Sautiere, P.; van Dorsselaer, A., *et al.* A corrected primary structure for the dog-fish Scylliorhinus caniculus protamine Z. *Biochem. Biophys. Acta*, **1993**, *1162*, 99-104.
[91] Kyu, T.; Ilies, I.; Shen, C.; Zhou, Z.L. In: *Liquid-Crystalline Polymer Systems: Technological Advances*; Isayev, A.I.; Kyu, T.; Cheng, S.Z.D., Eds.; American Chemical Society: Washington DC, USA, **1996**; pp. 201-215.
[92] Lin, Z.; Zhang, H.; Yang, Y. Spinodal decomposition kinetics of a mixture of liquid crystals and polymers. *Macromol. Chem. Phys.*, **1993**, *200*, 943-948.
[93] Jones, R.A.L. *Soft Condensed Matter*, Oxford University Press: Oxford, UK, **2002**.
[94] Harrison, L.G. *Kinetic Theory of Living Pattern*, Cambridge University Press: Cambridge, UK, **1993**.
[95] Harrison, L.G. *The Shaping of Life: A Kinetic Approach*, Cambridge University Press: Cambridge, UK, **2010**.
[96] Ward, S.W. Function of sperm chromatin structural elements in fertilization and development. *Mol. Hum. Reprod.*, **2010**, *16*, 30-36.
[97] Cerna, A.; Lopez-Fernandez, C.; Fernandez, J.L.; Moreno Diaz de la Espina, S.; de la Torre, C., *et al.* Triplex configuration in the nick-free DNAs that constitute the chromosomal scaffolds in grasshopper spermatids. *Chromosoma*, **2008**, *117*, 15-24.
[98] Ribes, E.; Gimenez-Bonafe, P.; Martinez-Soler, F.; Gonzalez, A.; Saperas, N., *et al*. Chromatin organization during spermiogenesis in Octopus vulgaris. I. morphological structures. *Mol. Reprod. Dev.*, **2004**, *68*, 223-231.
[99] Livolant, F.; Mangenot, S.; Leforestier, A.B.; de Frutos, M.; Raspaud, E., *et al*. Are liquid crystalline properties of nucleosomes involved in chromosome structure and dynamics? *Phil. Trans. R. Soc. Lond. A*, **2006**, *364*, 2615-2633.
[100] Chatchavalvanich, K.; Thongpan, A.; M., N. Ultrastructure of spermiogenesis in the freshwater stingray, Himantura signifer. *Ichthyol. Res.*, **2005**, *52*, 379-385.
[101] Stanley, H.P. Fine structure of spermiogenesis in the elasmobranch fish Squalus suckleyi. I. Acrosome formation, nuclear elongation and differentiation of the midpiece axis. *J. Ultrastruct. Res.*, **1971**, *36*, 86-102.
[102] Stanley, H.P. Fine structure of spermiogenesis in the elasmobranch fish Squalus suckleyi. II. Late stages of differentiation and structure of the mature spermatozoon. . *J. Ultrastruct. Res.*, **1971**, *36*, 103-118.
[103] Stanley, H.P.; Kasinsky, H.E.; Bols, N.C. Meiotic chromatin diminution in a vertebrate, the holocephalan fish Hydrolagus colliei (Chondrichthyes, Holocephali). *Tissue Cell*, **1984**, *16*, 203-215.
[104] Saperas, N.; Chiva, M.; Bols, N.C.; Kulak, D.; Kasinsky, H.E. Sperm-specific basic proteins in the holocephalan fish Hydrolagus colliei (Chondrichthyes, Chimaeriformes) and comparison with protamines from an elasmobranch. *Biol. Bull.*, **1993**, *185*, 186-196.
[105] Chiva, M.; Saperas, N.; Cáceres, C.; Ausió, J. In: *Advances in Spermatazoal Phylogeny and Taxonomy*; Jamieson, B.G.M.; Ausió, J.; Justine, J.L., Eds.; Memoires du Museum National d'Histoire Naturelle: Paris, France, **1995**; pp. 501-514.
[106] Muñoz, M.; Casadevall, M.; Bonet, S. Gametogenesis of Helicolenus dactylopterus dactylopterus (Teleostei, Scorpaenidae). *Sarsia*, **2002**, *87*, 119-127.
[107] Billard, R. Spermiogenesis in the rainbow trout (Salmo gairdneri). *Cell Tissue Res.*, **1983**, *233*, 265-284.
[108] Balhorn, R. In: *Molecular Biology of Chromosome Function*; Adolph, K.W., Ed Springer-Verlag: New York, USA, **1989**; pp. 366-395.
[109] Hud, N.V.; Vilfan, I.D. Toroidal DNA condensates: Unraveling the fine structure and the role of nucleation in determining size. *Annu. Rev. Biophys. Biomol. Struct.*, **2005**, *34*, 295-318.
[110] Gunton, J.D.; San Miguel, M.; Sahni, P.S. In: *Phase Transitions and Critical Phenomena*; Domb, C.; Lebowitz, C., Eds.; Academic Press: London, UK, **1983**; pp. 267-466.
[111] Fawcett, D.W.; Anderson, W.A.; Phillips, D.M. Morphogenetic factors influencing the shape of the sperm head. *Dev. Biol.*, **1971**, *26*, 220-251.
[112] Dooher, G.B.; Bennett, D. Fine structural observations on the development of the sperm head in the mouse. *Am. J. Anat.*, **1973**, *136*, 339-361.
[113] Kaye, J.S.; McMaster-Kaye, R. The fine structure and chemical composition of nuclei during spermiogenesis in the house cricket. *J. Cell Biol.*, **1966**, *31*, 159-179.
[114] Kaye, J.S.; McMaster-Kaye, R. In: *The Biology of the Male Gamete*; Duckett, J.G.; Racey, P.A., Eds.; Academic Press: New York, **1975**; pp. 227-237.
[115] Gompper, G.; Schick, M. In: *Phase Transitions and Critical Phenomena*; Domb, C.; Lebowitz, C., Eds.; Academic Press: London, UK, **1994**; pp. 3-176.
[116] Garcia-Ramirez, M.; Subirana, J.A. Condensation of DNA by basic proteins does not depend on protein composition. *Biopolymers*, **1994**, *34*, 285-292.
[117] Subirana, J.A. Order and disorder in 30 nm chromatin fibers. *FEBS Lett.*, **1992**, *302*, 105-107.
[118] Bloch, D.P.; Hew, H.Y.C. Schedule of spermatogenesis in the pulmonate snail Helix aspersa with special reference to histone transition. *J. Biophys. Biochem. Cytol.*, **1960**, *7*, 515-535.
[119] Dolder, H. In: *Advances in Spermatozoal Taxonomy and Phylogeny*; Jamieson, B.G.M.; Ausió, J.; Justine, J.L., Eds.; Memoires du Museum d´Histoire Naturelle: Paris, France, **1995**; pp. 285-289.
[120] Bloomfield, V.A. DNA condensation by multivalent cations. *Biopolymers*, **1997**, *44*, 269-282.
[121] Bertin, A.; Mangenot, S.; Renouard, M.; Durand, D.; Livolant, F. Structure and phase diagram of nucleosome core particles aggregated by multivalent cations. *Biophys. J.*, **2007**, *93*,
[122] Walker, M.H.; MacGregor, H.C. Spermatogenesis and the structure of the mature sperm in Nucella lapillus (L.). *J. Cell Sci.*, **1968**, *3*, 95-104.
[123] Gallardo, C.S.; Garrido, O.A. Spermiogenesis and sperm morphology in the marine gastropod Nucella crassilabrum with an account of morphometric patterns of spermatozoa variation in the family Muricidae. *Inv. Reprod. Dev.*, **1989**, *15*, 163-170.
[124] Jaramillo, R.; Garrido, O.; Jorquera, B. Ultrastructural analysis of spermiogenesis and sperm morphology in Chorus giganteus (Lesson, 1829) (Prosobranchia; Muricidae). *Veliger*, **1986**, *29*, 217-225.
[125] Ribes, E.; Sanchez De Romero, L.D.; Kasinsky, H.E.; Del Valle, L.; Gimenez-Bonafe, P., *et al.* Chromatin reorganization during spermiogenesis of the mollusc Thais hemostoma (Muricidae): implications for sperm nuclear morphogenesis in cenogastropods. *J. Exp. Zool.*, **2001**, *289*, 304-316.
[126] Buckland-Nicks, J.A.; Chia, F.-S. Spermatogenesis of a marine snail, Littorina sitkana. . *Cell Tissue Res.*, **1976**, *170*, 455-475.
[127] Kaye, J.S. Changes in the fine structure of nuclei during spermiogenesis. *J. Morphol.*, **1958**, *103*, 311-329.
[128] Rebhun, L.I. Nuclear changes during spermiogenesis in a pulmonate snail *J. Biophys. Biochem. Cytol.*, **1957**, *3*, 509-524.
[129] Fernandes, A.P.; Curi, G.; Francca, F.G.R.; Bao, S.N. Nuclear changes and acrosome formation during spermiogenesis in Euchistus heros (Hemiptera; Pentatomidae). *Tissue Cell*, **2001**, *33*, 286-293.
[130] Chevaillier, P.; Gusse, M. Evolution de la composition chimique et de la structure fine de la chromatine au cours de la spermiogenese

du criquet Locust migratoria. *J. Microsc. Biol. Cell.*, **1975**, *23*, 153-164.

[131] Sakai-Wada, A.; Hikita, Y. Ultrastructural studies on the chromatin fibers during spermiogenesis in the cockroach Blattella germanica. *Cytologia*, **1984**, *49*, 851-864.

[132] Jamieson, B.G.M.; Dallai, R.; Afzelius, B.A. *Insects: Their Spermatozoa and Phylogeny*, Science Publishers: Enfield, New Hampshire, USA, **1999**.

[133] Werner, G.; Werner, K. Changes in the nucleus, endoplasmic reticulum, Golgi apparatus, and acrosome during spermiogenesis in the waterstrider, Gerris najas Deg. (Heteroptera: Gerridae). *Int. J. Insect Morphol. Embryol.*, **1993**, *22*, 521-534.

[134] Baccetti, B.; Burrini, A.G.; Dallai, R.; Pallini, V.; Periti, P., *et al*. The spermatozoon of Arthropoda. XIX. Structure and function in the spermatozoon of Bacillus rossius. *J. Ultrastruct. Res.*, **1973**, *44*, 1-73.

[135] Wolf, K.W.; Klein, C. Development of the sperm head in the caddis fly Potamophylax rotundipennis (Insecta, Trichoptera). *Zoomorph.*, **1995**, *115*, 109-115.

[136] Bawa, S.R. Electron microscope study of spermiogenesis in a fire-brat insect, Thermobia domestica Pack. I. mature spermatozoon. *J. Cell Biol.*, **1964**, *23*, 431-446.

[137] Watson, N.A.; Rohde, K. Ultrastructure of spermiogenesis and spermatozoa in Phaenocora anomalocoela (Platyhelminthes, Typhloplanida, Phaenocorinae). *Inv. Reprod. Dev.*, **1994**, *25*, 237-246.

[138] Foata, J.; Culioli, J.-L.; Marchand, B. Ultrastructure of spermiogenesis and the spermatozoon of Macracanthorhynchus irudinaceus (Pallas, 1781) (Acanthocephala: Archiacanthocephala), a parasite of the wild boar Sus scrofa. *J. Parasitol.*, **2005**, *91*, 499-506.

[139] Pickett-Heaps, J.D. Ultrastructure and differentiation in Chara (fibrosa).IV. Spermatogenesis. *Aust. J. Biol. Sci.*, **1968**, *21*, 255-274.

[140] Kwiatkowska, M. Changes in ultrastructure of cytoplasm and nucleus during spermiogenesis in Chara vulgaris. *Folia Histochem. Cytobiol.*, **1996**, *34*, 41-56.

[141] Raikov, I.B. *The Protozoan Nucleus: Morphology and Evolution*, Springer Verlag: Vienna, **1982**.

[142] Van den Hoek, C.; Mann, D.G.; Jahns, H.M. *Algae: An Introduction to Phycology*, Cambridge University Press: Cambridge, UK, **1995**.

[143] Hausmann, K.; Hulsmann, N. *Protozoology*, Thieme Medical Publishers: New York, USA, **1996**.

[144] Jones, D.T.; Taylor, W.R.; Thornton, J.M. The rapid generation of mutation data matrices from protein sequences. *Comp. Appl. Biosci.*, **1992**, *8*, 275-282.

Received: March 16, 2010 **Revised: September 3, 2010** **Accepted: October 5, 2010**